# The novel pan-PIM kinase inhibitor, PIM447, displays dual anti-myeloma and bone protective effects, and potently synergizes with current standards of care

**Authors:** Teresa Paíno[1,2*], Antonio Garcia-Gomez[1,2*], Lorena González-Méndez[1,2], Laura San-Segundo[1,2], Susana Hernández-García[1,2], Ana-Alicia López-Iglesias[1,2], Esperanza M Algarín[1,2], Montserrat Martín-Sánchez[1,2], David Corbacho-González[3], Carlos Ortiz-de-Solorzano[3], Luis A Corchete[1,2], Norma C Gutiérrez[1,2], María-Victoria Mateos[1,2], Mercedes Garayoa[1,2#] and Enrique M Ocio[1,2#]

**Author affiliations:** (1) Centro de Investigación del Cáncer-IBMCC (CSIC-Universidad de Salamanca), Salamanca, Spain; (2) Complejo Asistencial Universitario de Salamanca-IBSAL, Salamanca, Spain; (3) Program in Solid Tumors and Biomarkers, Centro de Investigación Médica Aplicada (CIMA), Universidad de Navarra; Navarra's Health Research Institute (IDISNA), Pamplona, Spain

[*]Equal contribution

[#]Equal contribution

**Running title:** Preclinical activity of PIM447 in multiple myeloma

**Keywords:** Multiple myeloma, treatment, pan-PIM inhibitor, bone disease, drug combinations

**Financial support**

This work was supported by funding from the RTICC-Hematology Group (RD12/0036/0058), Spanish FIS (PI11/01465 and PI15/02156) and FEDER Funds, Ministerio de Economía y Competitividad grant DPI2012-38090-C03-02 (CO-D-S), AECC (GCB120981SAN), Junta de Castilla y León, Consejerías de Sanidad (GRS 862/A/13, GRS 1175/A/15 and BIO/SA05/14) y Educación

(FIC335U14) and the Centro en Red de Medicina Regenerativa y Terapia Celular de Castilla y León.

**Corresponding author:**

Enrique M. Ocio MD, PhD
Department of Hematology
Complejo Asistencial Universitario de Salamanca-IBSAL
Centro de Investigación del Cáncer-Universidad de Salamanca
Paseo de San Vicente, 58-182 37007 Salamanca, Spain
Phone: +34 923 291384 or +34 923 294812
Fax: +34 923 294624
e-mail: emocio@usal.es

**Conflict-of-interest disclosure**: EMO discloses research funding and consultancy for Novartis Pharmaceuticals. M-VM discloses consultancy for Novartis Pharmaceuticals. The remaining authors declare no competing interests.

Text word count: 4989
Abstract word count: 243
Number of figures: 6
Number of references: 46

## TRANSLATIONAL RELEVANCE

PIM kinases have been recently proposed as new therapeutic targets in oncology. PIM447 is the only pan-PIM kinase inhibitor that has reached clinical development in MM with promising preliminary efficacy results. In this work, we demonstrate through the use of preclinical models the potent anti-myeloma and bone protective effects of PIM447, and the mechanisms responsible of such effects. In addition, we show the very strong synergy exhibited by this drug in combination with different standard-of-care treatments. The preclinical efficacy of PIM447 demonstrated in the present work together with the preliminary single-agent efficacy and tolerable safety profile observed in the clinical setting, reinforces PIM inhibition as a promising therapeutic strategy in myeloma, and opens the door to new clinical trials with this drug.

## ABSTRACT

**Purpose:** PIM kinases are a family of serine/threonine kinases recently proposed as therapeutic targets in oncology. In the present work, we have investigated the effects of the novel pan-PIM kinase inhibitor, PIM447, on myeloma cells and myeloma-associated bone disease using different preclinical models.

**Experimental Design:** *In vitro*/*ex vivo* cytotoxicity of PIM447 was evaluated on myeloma cell lines and patient samples. Synergistic combinations with standard treatments were analyzed with Calcusyn Software. PIM447 effects on bone cells were assessed on osteogenic and osteoclastogenic cultures. The mechanisms of PIM447 were explored by immunoblotting, qPCR and immunofluorescence. A murine model of disseminated multiple myeloma was employed for *in vivo* studies.

**Results:** PIM447 is cytotoxic for myeloma cells due to cell cycle disruption and induction of apoptosis mediated by a decrease in phospho-Bad (Ser112) and c-Myc levels and the inhibition of mTORC1 pathway. Importantly, PIM447 demonstrates a very strong synergy with different standard treatments such as bortezomib + dexamethasone (combination index, CI=0.002), lenalidomide + dexamethasone (CI=0.065) and pomalidomide + dexamethasone (CI=0.077). PIM447 also inhibits *in vitro* osteoclast formation and resorption, downregulates key molecules involved in these processes and partially disrupts the F-actin ring, while increasing osteoblast activity and mineralization. Finally, PIM447 significantly reduced the tumor burden and prevented tumor-associated bone loss in a disseminated murine model of human myeloma.

**Conclusions:** Our results demonstrate dual anti-tumoral and bone protective effects of PIM447. This fact, together with the very strong synergy exhibited with standard-of-care treatments, supports the future clinical development of this drug in multiple myeloma.

## INTRODUCTION

Multiple myeloma (MM) is characterized by a proliferation of malignant plasma cells in the bone marrow (BM) that secrete a monoclonal immunoglobulin (1). It is typically associated with osteolytic lesions, due to an increase in the number and bone-resorptive activity of osteoclasts (OCs) together with osteoblast (OB) inhibition (2). Over the last decade, the introduction of new drugs, such as proteasome inhibitors and immunomodulatory agents, has improved the outcome of MM patients (3, 4); however, MM is still considered incurable mainly due to the development of drug resistance. Therefore, the identification of new targets and the investigation of novel drugs against such targets are extremely important for the discovery of more effective treatments (5).

Recently, PIM kinases have been proposed as being new therapeutic targets for treating hematological cancers (6). These are a family of serine/threonine kinases comprising three members (PIM1, PIM2 and PIM3), that regulate oncogenesis, survival pathways, drug resistance and migration, among other functions (7). Several features make PIM inhibition an attractive therapeutic strategy, particularly against myeloma cells: i) PIM2 is among the most highly over-expressed genes in MM cells (8), ii) this protein is required for maintaining MM cell growth (9), and iii) the expression of PIM2 in MM cells is enhanced by mesenchymal stromal cells (MSCs) and OCs as a survival and drug resistance mechanism (10). In addition, recent studies have also demonstrated the importance of PIM kinases in the biology of bone-remodeling cells. Accordingly, Kim and colleagues found that PIM1 positively regulates the ligand of the receptor activator of NF-κB (RANKL)-induced osteoclastogenesis (11). More recently, it has been shown that PIM2 acts as a negative regulator of

osteoblastogenesis (12). Based on all these data, it is tempting to hypothesize that the inhibition of these proteins would result not only in an anti-tumor activity, but may also have a beneficial effect on MM patients' bone disease.

PIM447 (N-(4-((1R,3S,5S)-3-amino-5-methylcyclohexyl)pyridin-3-yl)-6-(2,6-difluorophenyl)-5-fluoropicolinamide) is a potent and selective pan-PIM kinase inhibitor, derived from the tool compound LGB321 (6, 9), with pharmacokinetic and drug-like properties suitable for clinical development (13). In fact, preliminary results from a phase I clinical trial with PIM447 in patients with relapsed and/or refractory MM, have demonstrated single agent activity and a tolerable safety profile (14). Although the preclinical efficacy of other PIM inhibitors has been studied in several hematological malignancies including MM (12, 15-18), only two of them, SGI-1776 and AZD1208, have reached clinical trials but none in MM.

In the present work, we have investigated through the use of preclinical models, the activity and mechanism of action of PIM447 in myeloma cells, its potential synergism with standard-of-care treatments and its effects on myeloma-associated bone disease. To the best of our knowledge, this is the first clinical pan-PIM-inhibitor that demonstrates dual anti-myeloma and bone protective effects and this fact, together with the very strong synergy that PIM447 exhibits with standard-of-care treatments and the preliminary favorable clinical data, supports the future clinical development of this drug for the treatment of MM patients.

## MATERIALS AND METHODS

**Drugs.** PIM447 was provided by Novartis Pharmaceuticals, Inc. (Basel, Switzerland). Bortezomib was purchased from LC Laboratories (Woburn, MA, USA), lenalidomide and pomalidomide from Selleckchem (Houston, TX, USA) and dexamethasone from Sigma-Aldrich (St Louis, MO, USA).

**Cell lines, primary samples and cultures.** The human myeloma cell lines, MM1S, MM1R, U266 and NCI-H929 were purchased from ATCC (Manassas, VA, USA) whereas RPMI-8226 and OPM-2 were obtained from DSMZ (Braunschweig, Germany). The human myeloma cell line MM144 was a generous gift from Dr. S. Rudikoff (National Cancer Institute, National Institutes of Health, Bethesda, MD, USA). The source of the human myeloma cell lines RPMI-LR5, U266-Dox4 and U266-LR7 has been previously described (19). The origin of MM1S-luc and RPMI-8226-luc cells (luciferase-expressing) was previously explained (20). All myeloma cell lines were cultured as previously described (19). The MM1S-luc co-cultures with either the hMSC–TERT cell line (obtained from Dr. D. Campana, St. Jude Children's Research Hospital, Memphis, TN) or OCs were performed in the absence or presence of different concentrations of PIM447 as previously explained (20). Cell line identities have been tested and authenticated by short tandem repeat (STR) analysis with a PowerPlex 16 HS System Kit (Promega) and online STR matching analysis (DSMZ institute; available from: http:// www.dsmz.de/fp/register.php).

All primary bone marrow (BM) and peripheral blood samples were obtained after the approval of the Complejo Asistencial Universitario de Salamanca Review Board and with the written informed consent of all participating subjects.

**Cell viability, cell cycle and apoptosis assays.** Cell viability of myeloma cells was evaluated by the MTT method (19). The half-maximal inhibitory concentration ($IC_{50}$) of PIM447 was calculated using SigmaPlot graphing software. The cell cycle profile and apoptosis induction were evaluated as previously described (21).

***Ex vivo*** **analysis of apoptosis in freshly isolated patient cells.** BM samples from patients with MM were lysed and cultured as previously described (21), in the absence or presence of PIM447. The percentage of annexin-V positive cells was analyzed by flow cytometry on myelomatous PCs ($CD38^{+bright}$, $CD45^{-/low}$, $SSC^{low/intermediate}$, $CD56^{-/+}$) and normal lymphocytes ($CD45^{++}$, $SSC^{low}$) populations.

**Evaluation of the potential synergism of PIM447 with other anti-myeloma agents.** MM1S or RPMI-8226 cells were treated for 48-72 h with double and triple combinations of PIM447 and other anti-myeloma agents (bortezomib, lenalidomide, pomalidomide and dexamethasone). Cell viability was analyzed by MTT assays. The potency of each combination was quantified with Calcusyn software (Biosoft, Ferguson, MO, USA), which is based on the Chou Talalay method, yielding a combination index (CI) with the following interpretation: CI>1, antagonistic effect; CI=1, additive effect; CI<1, synergistic effect.

***In vitro*** **OC formation, resorption pits and integrity of F-actin ring.** Peripheral blood mononuclear cells (PBMCs) from healthy donors were differentiated in osteoclastogenic medium (containing 25 ng/mL M-CSF and 50 ng/mL RANKL, both from Peprotech) as previously described (22). Assays related to OCs formation and function included: F-actin ring formation (pre-OCs,

14 days differentiation), resorption capacity (17 days differentiation), and OC formation (21 days differentiation), and were performed as previously reported (23).

***In vitro* OB differentiation, alkaline phosphatase activity and mineralization assays.** OBs were generated and assayed as previously described (20). Briefly, primary MSCs (passage 2-3) were cultured in osteogenic medium (containing 5 mM β-glycerophosphate and 50 mg/mL ascorbic acid) and exposed to PIM447. After 11 days, alkaline phosphatase (ALP) activity was quantified by hydrolysis of p-nitrophenylphosphate into p-nitrophenol (Sigma-Aldrich), whereas mineralization was assessed by Alizarin Red staining of calcium deposits at day 21.

**Gene expression data: source, processing and analysis.** All gene expression microarray datasets were retrieved from Gene Expression Omnibus (http://www.ncbi.nlm.nih.gov/geo/, accession number: GSE47552) (24). CEL files were background-corrected and normalized using the Robust Multi-Array (RMA) algorithm implemented in the Affymetrix Expression Console, to estimate the $\log_2$ normalized expression values for PIM1, PIM2 and PIM3.

**Immunoblotting.** Western blot was performed following standard procedures (25). Phospho-TSC2 levels were examined with a specific phospho-Akt substrate antibody (Cell Signaling Technology; Boston, MA, USA) following TSC2 immunoprecipitation, as previously described (9). The origin of primary antibodies was as follows: anti-Bcl-2, anti-Mcl-1, anti-p-Erk1/2, anti-NFATc1 and anti-cathepsin K from Santa Cruz Biotechnology (Santa Cruz, CA, USA); α-tubulin from Calbiochem (Billerica, MA, USA); all other antibodies from Cell

Signaling Technology. The horseradish peroxidase-conjugated secondary antibodies were from GE Healthcare (Little Chalfont, UK).

**Reverse transcription real-time PCR analyses.** Total RNA was isolated using TRIzol reagent (Invitrogen). TaqMan Gene Expression Assays (Applied Biosystems, Waltham, MA USA) were performed according to the manufacturer's instructions: *CA2* (Hs00163869_m1), *ATP6V1A* (Hs01097169_m1) and *MMP9* (Hs00234579_m1). Normalized gene expression was calculated as $2^{-\Delta Ct}$, being $\Delta Ct$ = Ct (gene) – Ct (GAPDH).

**Mouse model of bone marrow-disseminated human multiple myeloma**. Animal experiments were conducted according to institutional guidelines for the use of laboratory animals, and after granted permission from the University of Salamanca Animal Ethical Committee for animal experimentation. RPMI-8226-luc cells ($8 \times 10^6$) were injected intravenously into 6-week-old female NOD-SCID-IL-2R$\gamma^{-/-}$ (NSG) mice (Charles River Laboratories, Wilmington, MA, USA) and tumor development was monitored by noninvasive bioluminescence imaging (BLI), as previously described (20). After 4 weeks, animals were randomized into two groups (n=12/group), one receiving vehicle (5 times/week by oral gavage), the other receiving PIM447 (100 mg/kg, 5 times/week by oral gavage). Serum levels of human Ig$\lambda$ (secreted by RPMI-8226-luc cells) were determined by ELISA (Bethyl Laboratories, Montgomery, TX, USA). For microcomputed tomography (microCT) analysis, one femur of each animal was fixed in 10% formalin and scanned using a microCT system (MicroCATII; Siemens) as described previously (22). The trabecular microarchitecture in the distal femur was analyzed using BoneJ (26). Carboxy-terminal telopeptide

collagen cross-links (CTX) and N-terminal propeptide of type I procollagen (P1NP) were measured in mice sera by ELISA (Immunodiagnostic Systems, Boldon, Tyne & Wear, UK).

**Statistical analyses.** Statistical analyses were performed using SPSS-v21.0 software (IBM Corp., Armonk, NY, USA).

## RESULTS

**PIM kinases are expressed in MM cell lines and myeloma cells from patients.** We initially evaluated the basal levels of PIM kinases in MM cell lines and primary myeloma cells. As shown in Figure 1a, the three isoforms (PIM1, PIM2 and PIM3) were expressed in the 10 MM cell lines analyzed. Notably, the level of expression of PIM2 was higher than the other two PIM kinases. Consistent with these results, we also observed in a series of 41 patients with newly-diagnosed MM that PIM2 levels were significantly higher than PIM1 and PIM3 in CD138+ myeloma cells (Figure 1b). In addition, PIM1 levels were significantly higher than PIM3 levels (Figure 1b).

**PIM447 is cytotoxic for MM cells and overcomes the resistance conferred by MSCs and OCs.** Since PIM kinases are highly expressed in MM cells, we evaluated the anti-myeloma effect of the new pan-PIM kinase inhibitor, PIM447. Different MM cell lines were treated with increasing concentrations of PIM447 (0.05-10 μM) for 24, 48 and 72 h. The dose-response curves obtained by MTT assay revealed two patterns of sensitivity: sensitive cell lines with $IC_{50}$ values at 48 h ranging from 0.2 to 3.3 μM (MM1S, MM1R, RPMI-8226, MM144, U266 and NCI-H929) and less sensitive cell lines with $IC_{50}$ values at 48 h >7 μM (OPM-2,

RPMI-LR5, U266-Dox4 and U266-LR7) (Figure 1c). A lack of correlation was found between the levels of PIM kinases and the $IC_{50}$ values for PIM447 ($p$>0.05) (Figure 1d). To explore the induction of apoptosis, three of the sensitive cell lines (MM1S, NCI-H929 and RPMI-8226) and two of the less sensitive cell lines (OPM-2 and RPMI-LR5) were treated with increasing doses of PIM447 for 24 and 48 hours (Figure 2a), revealing a clear dose-response: while low doses of the drug (0.1-1 μM) did not induce important levels of apoptosis in any of the cell lines tested, PIM447 at 5 μM substantially increased annexin-V levels (about 30%) in sensitive cell lines but not in OPM-2 and RPMI-LR5. In addition, the highest dose (10 μM) induced apoptosis in all the cell lines but to a lesser extent in OPM-2 and RPMI-LR5. When MM1S cells were treated with 10 μM PIM447 for different times, we observed a time-dependent increase in apoptotic cells (Figure 2b). Moreover, treatment of MM1S cells with PIM447 promoted the cleavage of initiator caspases, such as caspases 8 and 9, and also the cleavage of the effector caspases 3 and 7, together with PARP cleavage (Figure 2c). Similar results were found in RPMI-8226 and NCI-H929 cells (Supplementary Figure 1a-b). To assess the potential effect of PIM447 on cell cycle, MM1S and OPM-2 cells were incubated with increasing concentrations (0.1-10 μM) of this drug for 48 hours, and the cell cycle was analyzed by flow cytometry. PIM447 increased the percentage of cells in the $G_0/G_1$ phase and decreased the proliferative phases (S and $G_2$/M) of the cell cycle, in the two cell lines at all doses (Figure 2d). Nevertheless, the effects at low concentrations (0.1-1 μM) were more pronounced in MM1S cells than in OPM-2. Accordingly, the increase in the percentage of cells in $G_0/G_1$ after treatment with 0.1, 0.5 or 1 μM PIM447 was, respectively, 10.2%, 16.66% and

19.18% in MM1S; and 6.54%, 11.09% and 9.51% in OPM-2. Similar results to those of MM1S were found in NCI-H929 (Supplementary Figure 1c). Overall, these results indicate that, at least at low doses of the drug, OPM-2 cells are less susceptible to cell cycle effects than sensitive cell lines.

The effect of PIM447 was also investigated *ex vivo* in cells isolated from BM samples from 10 patients with MM, as explained in Methods. After 48 h of exposure, PIM447 clearly induced apoptosis in myeloma cells (concentrations in the 5-10 μM range) with low to moderate toxicity in lymphocytes (Figure 2e).

Finally, we investigated whether PIM447 could overcome the protective effect conferred by the BM microenvironment on MM cells. For this purpose, MM1S-luc cells were co-cultured with MSCs or OCs in the presence of PIM447. Despite the proliferative advantage conferred by MSCs and OCs, PIM447 greatly reduced the viability of MM cells under these circumstances (Figure 2f).

**PIM447 potentiates the efficacy of various anti-myeloma agents.** Since current treatment of MM is largely based on combinations of drugs with different mechanisms of action, we studied the effect of combining PIM447 with several standard-of-care treatments in MM. The potency of each combination in MM1S cells was analyzed with Calcusyn software. With respect to double combinations, the synergy (CI<1) of PIM447 with dexamethasone, lenalidomide and pomalidomide is noticeable (Figure 3a-c and Supplementary Tables 1, 2 and 3), being the combination with dexamethasone in the highly synergistic range (CI=0.096) at PIM447 200 nM + dexamethasone 10 nM (Figure 3a and Supplementary Table 1). On the other hand, triple combinations of PIM447 with bortezomib + dexamethasone (Figure 3a and Supplementary Table 1),

lenalidomide + dexamethasone (Figure 3b and Supplementary Table 2) and pomalidomide + dexamethasone (Figure 3c and Supplementary Table 3) also showed a very strong synergism. To confirm these results, the same combinations were tested on the RPMI-8226 cell line, rendering similar results (Supplementary Figure 2).

**Effect of PIM447 on PIM kinase-related targets.** PIM kinases are known to directly phosphorylate and regulate the pro-apoptotic Bcl-2 family member, Bad (27-29). Accordingly, treatment of MM1S, RPMI-8226 and NCI-H929 cells with 10 μM PIM447 for different times reduced the phosphorylation of Bad on Ser112 without affecting the levels of total Bad (Figure 4a and Supplementary Figure 3a). In addition, treatment of MM1S cells with PIM447 reduced the levels of the Bad-regulated antiapoptotic protein Bcl-xl, but did not modify the levels of other antiapoptotic Bcl-2 family members such as Bcl-2 and Mcl-1 (Figure 4a).

PIM2 modulates mTORC1 activity and promotes myeloma cell proliferation through phosphorylation of TSC2 (9). In this regard, just 1 hour of treatment with PIM447 strongly inhibited the phosphorylation of TSC2 in MM1S cells, whereas the phosphorylation of PRAS40, another mTORC1 modulator, at Thr246 required longer exposure (24 h) to produce a decrease (Figure 4b). In addition, treatment of MM1S cells with PIM447 reduced the phosphorylation of downstream mTORC1 targets such as 4EBP1 at Thr 37/46, P70S6 at Thr 389 and S6RP at Ser 235/236 (Figure 4b). Similar results were found for RPMI-8226 and NCI-H929 cells (Supplementary Figure 3b).

To gain further insights into the mechanism of PIM447, we analyzed c-Myc, a PIM-regulated transcription factor (30). Treatment of MM1S cells with PIM447

reduced the levels of total c-Myc and phospho-c-Myc at Ser62, a key residue involved in c-Myc stabilization (30) (Figure 4c). The levels of phospho-c-Myc (Ser62) also decreased in RPMI-8226 and NCI-H929 cells after treatment with PIM447 (Supplementary Figure 3c). Additionally, the levels of Mad-1, a protein that antagonizes Myc-mediated transcriptional activity, increased in MM1S after PIM447 exposure (Figure 4c). Treatment of MM1S cells with PIM447 also reduced the levels of cyclins D2 and E1, two well-known regulators of $G_1$-to-S phase transition, previously described as being transcriptionally induced by c-Myc (31-33) (Figure 4c).

As previously commented, the sensitivity to PIM447 differs among different MM cell lines. In order to elucidate the molecular basis for these differences, we explored the molecular effects of PIM447 in the low sensitive cell line OPM-2. Treatment of OPM-2 with 10 μM PIM447 reduced the levels of phospho-S6RP (Ser 235/236) and phospho-4EBP1 (Thr 37/46) after just 1 hour of treatment, indicating the inhibition of the mTORC1 pathway (Supplementary Figure 3d). Interestingly, PIM447 did not reduce the levels of phospho-Bad (Ser112) in OPM-2, whereas c-Myc and phospho-c-Myc (Ser62) only decreased after 24 hours of exposure to the drug (Figure 4d). Since the effects of PIM447 on these proteins were detected earlier in sensitive cell lines, we then analyzed the potential correlation between their basal levels in MM cell lines and the sensitivity to PIM447. The analysis showed a strong positive correlation between basal levels of Bad and the $IC_{50}$ for PIM447 ($r = 0.8880$; $p = 0.0006$. Figure 4e). A positive correlation was also found between basal levels of phospho-Bad and $IC_{50}$ values, although in this case the correlation was not so strong ($r = 0.6044$; $p = 0.0642$. Figure 4f). Finally, sensitivity to PIM447 does not

seem to be associated with basal levels of c-Myc (r = 0.4222; *p* = 0.2242) or phospho-c-Myc (r = 0.4270; *p* = 0.2184) (Supplementary Figure 4a-b).

**PIM447 inhibits osteoclastogenesis and bone resorption while increasing osteoblast activity and mineralization *in vitro*.** Since PIM1 is known to be involved in murine RANKL-induced osteoclastogenesis (11), we investigated the effect of PIM447 on the formation and function of OCs from human origin. First of all, we observed an upregulation of PIM1 and PIM3 during OC differentiation (Figure 5a). To evaluate the effect of PIM447 on OC formation, human PBMCs were exposed to several concentrations of the drug during OC differentiation. PIM447 reduced the number of $TRAP^+$ multinucleated cells ($IC_{50}$=2 μM) derived from PBMCs of healthy donors (Figure 5b). Moreover, representative micrographs in Figure 5b illustrate that cell densities were not significantly reduced in cultures exposed to up to 5 μM PIM447, suggesting a selective effect of PIM447 on inhibition of OC formation rather than on cell viability.

To evaluate changes in OC functionality, we examined the effect of PIM447 on osteoclastogenic cultures established on calcium substrate-coated slides. A dose-dependent reduction of the area of resorptive pits was observed with PIM447 treatment (Figure 5c). Of note, PIM447 inhibited OC-mediated resorption at doses clearly lower than those required to inhibit OC formation, suggesting that this drug not only inhibits osteoclastogenesis but also directly affects OC functionality.

To gain insight into the mechanisms mediating the aforementioned effects, we tested the effect of PIM447 on different transcription factors/molecules involved

in OC differentiation and activity. Although levels of PU.1 and p-ERK1/2 were not significantly modified, PIM447 treatment reduced the levels of NFATc1, a master transcription factor in the differentiation of OCs, and cathepsin K, a protease responsible for degradation of organic bone matrix (Figure 5d). We also observed that pre-OCs differentiated under PIM447 exposure were associated with partial disruption of the F-actin ring (Figure 5e). Expression of molecules involved in matrix resorption, such as the matrix metalloproteinase 9 (*MMP9*) and the vacuolar-$H^+$-ATPase catalytic subunit A1 (*ATP6V1A*) were significantly diminished after PIM447 treatment (Figure 5f), therefore stating the role of PIM447 in preventing bone resorption. Expression of carbonic anhydrase II (*CA2*) also decreased although not reaching statistical significance.

Since PIM2 has recently been identified as a negative regulator for osteoblastogenesis in MM and as an important target for treatment in myeloma bone disease (12), we also evaluated whether PIM447 was capable of promoting *in vitro* OB differentiation and activity. Primary MSCs from myeloma patients (n=5) were maintained in osteogenic medium in the presence of different PIM447 concentrations, and ALP activity was measured at day 11 as a surrogate marker of early OB function. As seen in Figure 5g, a significant increment in ALP activity was observed after treatment with the pan-PIM kinase inhibitor. We also observed a modest increase in matrix mineralization at the end of the osteogenic differentiation period (day 21) as assessed by Alizarin Red staining of calcium deposits (Figure 5h).

**PIM447 reduces tumor burden and prevents myeloma-associated bone loss in a mouse model of disseminated MM.** We examined whether the *in vitro* effects of PIM447 were also present *in vivo* in a disseminated murine

model of human myeloma. Compared with the vehicle group, PIM447 clearly controlled tumor progression as measured by bioluminescence (Figure 6a) and serum levels of hIgλ secreted by RPMI-8226-luc cells (Figure 6b). Importantly, PIM447 was well tolerated, as the body weight of mice did not decrease by more than 10% (Supplementary Figure 5).

Representative microCT images at the metaphysis of distal femurs showed tumor-associated bone loss in vehicle mice compared with normal bone (mice not injected with myeloma cells); in contrast, PIM447-treated animals showed a trabecular microarchitecture similar to that of normal bone (Figure 6c). Moreover, the analysis of bone morphometric parameters indicated that PIM447 increased bone volume density and trabecular number and reduced trabecular separation relative to vehicle control (Figure 6d). In accordance with these findings, the serum levels of the bone resorption marker CTX were significantly diminished in PIM447-treated mice (Figure 6e). Although there was a trend for PIM447 augmenting serum levels of the bone formation marker P1NP with respect to the vehicle-treated group, this was in the limit of statistical significance ($p$=0.06) (Figure 6f).

## DISCUSSION

The search for new targets is of utmost importance in MM because the disease is still incurable and the therapeutic options currently available are limited. PIM kinases are a family of serine/threonine kinases composed of three members (PIM1, PIM2 and PIM3) that have recently been proposed as new therapeutic targets in MM (6). Specifically, PIM2 is one of the most highly overexpressed

genes in MM (8) and its role as an antiapoptotic and cell growth mediator in myeloma cells has been described (9, 10). In line with these data, our results demonstrate that the level of expression of PIM2 in myeloma cells is higher than the expression of PIM1 and PIM3, suggesting that PIM2 has a major role in the biology of MM. Nevertheless, the three PIM kinases have shown some functional redundancy in transgenic Eμ-myc mice (34, 35). Since the functional overlap of PIM isoforms is also likely to occur in myeloma, it is reasonable to hypothesize that the use of pan-PIM inhibitors may be more effective than targeting individual isoforms. In this work, we have evaluated in preclinical models the efficacy of the novel pan-PIM kinase inhibitor, PIM447, in myeloma cells and bone disease.

PIM447 shows anti-myeloma activity in primary myeloma cells and MM cell lines, with different degrees of sensitivity. It is of note that these differences do not depend exclusively on basal levels of PIM kinases, since we found a lack of correlation between the expression of these proteins and the $IC_{50}$ values for PIM447. On the other hand, interactions between myeloma cells and their microenvironment are a crucial factor in myeloma growth and drug resistance (36). Here, we have shown *in vitro* that PIM447 reduces myeloma cell viability even in the presence of MSCs and OCs, suggesting that this drug is able to overcome microenvironment-mediated drug resistance. Moreover, the clear anti-tumoral effect of PIM447 observed in the *in vivo* murine model of disseminated MM, demonstrates the efficacy of this agent in the context of the BM microenvironment.

PIM kinases phosphorylate and regulate multiple targets involved in different functions such as cell cycle, apoptosis and metastasis (7). Our results with MM

cell lines and patient samples indicate that the cytotoxic effects of PIM447 are mediated through cell cycle disruption and induction of apoptosis. The effects at low doses of the drug are mainly due to cell cycle arrest rather than apoptosis induction, what is concordant with the clinical data, as many of the patients treated with the drug in monotherapy achieved stabilization of the disease, being some of them quite durable (14). Treatment of myeloma cells with PIM447 provokes an increase of cell cycle $G_0/G_1$ phase and a decrease of S phase, suggesting a cell cycle blockade at the $G_1$-to-S transition. Moreover, PIM447 also downregulates the expression of cyclins D2 and E1, two fundamental regulators of G1-to-S phase progression (37, 38). In addition, PIM447 reduced the levels of the transcription factor c-Myc, a direct target of PIM kinases (7), and increased the expression Mad-1, a protein that antagonizes Myc-mediated transcriptional activity (39). Since cyclins D2 and E1 have been described in fibroblast models to be transcriptionally induced by c-Myc (31-33), it is reasonable to speculate that the reduced expression of these cyclins after treatment with PIM447 may be a consequence of the reduction of c-Myc levels.

In addition to cell cycle blockade, the mechanism of PIM447 in myeloma involves the induction of apoptosis, as indicated by the increase of annexin-V positive cells after treatment, and the cleavage of caspases and their substrate, PARP. It should be noted, however, that the levels of apoptosis are quite moderate in less sensitive *versus* sensitive cell lines, even at high doses and long times of exposure to the drug. It is well established that PIM kinases phosphorylate Bad at Ser112 as an antiapoptotic mechanism (27, 28). Accordingly, treatment of sensitive MM cell lines with PIM447 reduced phospho-

Bad (Ser112) levels, suggesting that apoptosis induction is mediated, at least in part, by dephosphorylated Bad which is known to bind and thereby inactivate the antiapoptotic proteins Bcl-2 and Bcl-xl (40). In addition, treatment with PIM447 also reduced Bcl-xl levels in MM1S, but not Mcl-1 which has been shown to be downregulated by PIM inhibition in CLL and MCL (15, 41). On the contrary, the levels of phospho-Bad (Ser112) did not decrease after treatment with PIM447 in less sensitive cells, suggesting a potential mechanism for apoptosis resistance. Moreover, our results indicate that basal levels of Bad and phospho-Bad could predict the sensitivity to PIM447, since a positive correlation was found between basal levels of these proteins and the $IC_{50}$ values. Although there is no clinical information validating this correlation, the results here presented strongly support the study of changes induced in the phosphorylation of Bad as a potential biomarker of response to this family of agents.

Together with the described mechanisms, our results also indicate that PIM447 represses mTORC1 signaling in myeloma cells. In this regard, treatment with PIM447 reduces the phosphorylation of TSC2 and PRAS40, two mTORC1 inhibitors in their unphosphorylated state (42, 43). The effect on phospho-TSC2 was detected earlier than the effect on phospho-PRAS40, suggesting that PIM447 primarily modulates mTORC1 activity in myeloma cells through TSC2 (9). As a result of mTORC1 inhibition, there was a decrease in phospho-4EBP1 and phospho-P70S6, two of its downstream targets implicated in the translation of proteins involved in survival, cell cycle progression and the translation machinery itself (42, 43). These results indicate that the inhibition of protein translation would contribute to PIM447-induced cell death, as previously observed with other PIM inhibitors (15-17, 44).

A second major finding of our work is the beneficial effect of PIM447 on myeloma bone disease. It is known that the interaction between myeloma cells and their microenvironment contributes to bone disease as a consequence of increased osteoclastogenesis and suppressed osteoblastogenesis (45). Moreover, osteolytic lesions are the most common complications of myeloma, developing in more than 80% of patients, and associated with decreased overall survival (46). This highlights the importance of finding treatments not only targeting malignant plasma cells but also having a beneficial effect on bone disease. On the one hand, it has been reported that PIM1 positively regulates RANKL-induced murine osteoclastogenesis via NFATc1 induction (11). In this work, we have shown that both PIM1 and PIM3 expression increase during OC differentiation from human PBMCs and, consequently, our *in vitro* experiments show that PIM447 inhibits OC formation and resorptive activity. Mechanistically, these effects seem to be mediated, at least in part, by disruption of the F-actin ring and downregulation of several molecules involved in OC differentiation and function, including NFATc1, the major transcription factor integrating RANKL signaling in terminal OC differentiation. On the other hand, PIM2 expression has been found to be upregulated in bone marrow MSCs and pre-OBs from myeloma patients in the presence of inhibitory factors of osteoblastogenesis in myeloma (i.e. IL3, IL7, TNFα, TGFβ, activin A) or after co-culture with MM cells, and PIM2 inhibition was able to resume *in vitro* osteoblastogenesis (12). In accordance with the later results, PIM447 treatment of MSCs from myeloma patients also significantly increased ALP activity and augmented mineralization in *in vitro* assays. These *in vitro* effects on bone had their correlate in our mouse model of disseminated MM. As observed in the microCT images, the

bone trabecular architecture at the metaphyses of distal femurs in PIM447-treated animals was similar to that of normal bone. In fact, these results match with significantly augmented bone parameters of bone volume density and trabecular number and reduced trabecular separation. Moreover, significantly lower serum levels of CTX (bone resorption marker) were observed in PIM447-treated animals than in the vehicle control, being indicative of an *in vivo* effect of this drug in reducing OC resorptive activity. PIM447 also augmented levels of the bone formation marker P1NP with respect to those mice treated with vehicle, although differences did not reach statistical significance. Taken together, our data seem to be indicative of PIM447 having anti-myeloma activity and preventing bone loss, by both anti-resorptive and bone-anabolic effects. This is in line with previous reports showing that PIM2 kinase is an important target of treatment for tumor progression and bone loss in myeloma (12).

One final important point is the very strong synergistic effect observed when PIM447 is combined with standard treatments such as dexamethasone, bortezomib + dexamethasone, lenalidomide + dexamethasone and pomalidomide + dexamethasone. This makes this drug attractive to try to improve the efficacy of these standards of care, particularly with oral agents, as it would result in effective all-oral combinations.

Our preclinical results demonstrate the relevance of the new pan-PIM-kinase inhibitor, PIM447, in MM as shown by the dual anti-tumoral and bone protective effects displayed by this drug. Moreover, in addition to these beneficial effects, PIM447 strongly synergizes *in vitro* with standard-of-care treatments. In summary, the present work supports the use of PIM447 in MM patients, particularly in combination with the current standards of care.

## AUTHORSHIP

TP, AGG, MG and EMO designed research and wrote the paper. TP, AGG, LGM, LSS, SHG, AALI, EMA, MMS, DCG and CODS performed experiments and analyzed the data. LAC and NCG analyzed microarray data. MVM and EMO provided clinical samples and contributed to the clinical data. All authors reviewed and approved the manuscript.

## ACKNOWLEDGEMENTS

The authors thank Phil Mason for his help in reviewing English grammar.

## REFERENCES

1. Rollig C, Knop S, Bornhauser M. Multiple myeloma. Lancet 2015;385: 2197-208.

2. Raje N, Roodman GD. Advances in the biology and treatment of bone disease in multiple myeloma. Clin Cancer Res 2011;17: 1278-86.

3. Kumar SK, Rajkumar SV, Dispenzieri A, Lacy MQ, Hayman SR, Buadi FK*, et al.* Improved survival in multiple myeloma and the impact of novel therapies. Blood 2008;111: 2516-20.

4. Kumar SK, Dispenzieri A, Lacy MQ, Gertz MA, Buadi FK, Pandey S*, et al.* Continued improvement in survival in multiple myeloma: changes in early mortality and outcomes in older patients. Leukemia 2014;28: 1122-8.

5. Ocio EM, Richardson PG, Rajkumar SV, Palumbo A, Mateos MV, Orlowski R*, et al.* New drugs and novel mechanisms of action in multiple

myeloma in 2013: a report from the International Myeloma Working Group (IMWG). Leukemia 2014;28: 525-42.

6. Garcia PD, Langowski JL, Wang Y, Chen M, Castillo J, Fanton C*, et al.* Pan-PIM kinase inhibition provides a novel therapy for treating hematologic cancers. Clin Cancer Res 2014;20: 1834-45.

7. Blanco-Aparicio C, Carnero A. Pim kinases in cancer: diagnostic, prognostic and treatment opportunities. Biochem Pharmacol 2013;85: 629-43.

8. Claudio JO, Masih-Khan E, Tang H, Goncalves J, Voralia M, Li ZH*, et al.* A molecular compendium of genes expressed in multiple myeloma. Blood 2002;100: 2175-86.

9. Lu J, Zavorotinskaya T, Dai Y, Niu XH, Castillo J, Sim J*, et al.* Pim2 is required for maintaining multiple myeloma cell growth through modulating TSC2 phosphorylation. Blood 2013;122: 1610-20.

10. Asano J, Nakano A, Oda A, Amou H, Hiasa M, Takeuchi K*, et al.* The serine/threonine kinase Pim-2 is a novel anti-apoptotic mediator in myeloma cells. Leukemia 2011;25: 1182-8.

11. Kim K, Kim JH, Youn BU, Jin HM, Kim N. Pim-1 regulates RANKL-induced osteoclastogenesis via NF-kappaB activation and NFATc1 induction. J Immunol 2010;185: 7460-6.

12. Hiasa M, Teramachi J, Oda A, Amachi R, Harada T, Nakamura S*, et al.* Pim-2 kinase is an important target of treatment for tumor progression and bone loss in myeloma. Leukemia 2015;29: 207-17.

13. Burger MT, Nishiguchi G, Han W, Lan J, Simmons R, Atallah G*, et al.* Identification of N-(4-((1R,3S,5S)-3-Amino-5-methylcyclohexyl)pyridin-3-yl)-6-(2,6-difluorophenyl)- 5-fluoropicolinamide (PIM447), a Potent and Selective

Proviral Insertion Site of Moloney Murine Leukemia (PIM) 1, 2, and 3 Kinase Inhibitor in Clinical Trials for Hematological Malignancies. J Med Chem 2015;58: 8373-86.

14. Raab MS, Ocio EM, Thomas SK, Günther A, Goh YT, Lebovic D, Jakubowiak A, Song D, Xiang F, Patel A, Vanasse KG, Kumar S. Phase 1 Study Update of the Novel Pan-Pim Kinase Inhibitor LGH447 in Patients with Relapsed/ Refractory Multiple Myeloma. ASH 2014 Annual Meeting Abstract 301 2014.

15. Yang Q, Chen LS, Neelapu SS, Miranda RN, Medeiros LJ, Gandhi V. Transcription and translation are primary targets of Pim kinase inhibitor SGI-1776 in mantle cell lymphoma. Blood 2012;120: 3491-500.

16. Cervantes-Gomez F, Chen LS, Orlowski RZ, Gandhi V. Biological effects of the Pim kinase inhibitor, SGI-1776, in multiple myeloma. Clin Lymphoma Myeloma Leuk 2013;13 Suppl 2: S317-29.

17. Keeton EK, McEachern K, Dillman KS, Palakurthi S, Cao Y, Grondine MR*, et al.* AZD1208, a potent and selective pan-Pim kinase inhibitor, demonstrates efficacy in preclinical models of acute myeloid leukemia. Blood 2014;123: 905-13.

18. Meja K, Stengel C, Sellar R, Huszar D, Davies BR, Gale RE*, et al.* PIM and AKT kinase inhibitors show synergistic cytotoxicity in acute myeloid leukaemia that is associated with convergence on mTOR and MCL1 pathways. Br J Haematol 2014;167: 69-79.

19. Paino T, Sarasquete ME, Paiva B, Krzeminski P, San-Segundo L, Corchete LA*, et al.* Phenotypic, genomic and functional characterization reveals

no differences between CD138++ and CD138low subpopulations in multiple myeloma cell lines. PLoS One 2014;9: e92378.

20. Garcia-Gomez A, Quwaider D, Canavese M, Ocio EM, Tian Z, Blanco JF*, et al.* Preclinical activity of the oral proteasome inhibitor MLN9708 in Myeloma bone disease. Clin Cancer Res 2014;20: 1542-54.

21. Ocio EM, Maiso P, Chen X, Garayoa M, Alvarez-Fernandez S, San-Segundo L*, et al.* Zalypsis: a novel marine-derived compound with potent antimyeloma activity that reveals high sensitivity of malignant plasma cells to DNA double-strand breaks. Blood 2009;113: 3781-91.

22. Garcia-Gomez A, Ocio EM, Crusoe E, Santamaria C, Hernandez-Campo P, Blanco JF*, et al.* Dasatinib as a bone-modifying agent: anabolic and anti-resorptive effects. PLoS One 2012;7: e34914.

23. Hurchla MA, Garcia-Gomez A, Hornick MC, Ocio EM, Li A, Blanco JF*, et al.* The epoxyketone-based proteasome inhibitors carfilzomib and orally bioavailable oprozomib have anti-resorptive and bone-anabolic activity in addition to anti-myeloma effects. Leukemia 2013;27: 430-40.

24. Lopez-Corral L, Corchete LA, Sarasquete ME, Mateos MV, Garcia-Sanz R, Ferminan E*, et al.* Transcriptome analysis reveals molecular profiles associated with evolving steps of monoclonal gammopathies. Haematologica 2014;99: 1365-72.

25. Maiso P, Carvajal-Vergara X, Ocio EM, Lopez-Perez R, Mateo G, Gutierrez N*, et al.* The histone deacetylase inhibitor LBH589 is a potent antimyeloma agent that overcomes drug resistance. Cancer Res 2006;66: 5781-9.

26. Doube M, Klosowski MM, Arganda-Carreras I, Cordelieres FP, Dougherty RP, Jackson JS*, et al.* BoneJ: Free and extensible bone image analysis in ImageJ. Bone 2010;47: 1076-9.

27. Yan B, Zemskova M, Holder S, Chin V, Kraft A, Koskinen PJ*, et al.* The PIM-2 kinase phosphorylates BAD on serine 112 and reverses BAD-induced cell death. J Biol Chem 2003;278: 45358-67.

28. Aho TL, Sandholm J, Peltola KJ, Mankonen HP, Lilly M, Koskinen PJ. Pim-1 kinase promotes inactivation of the pro-apoptotic Bad protein by phosphorylating it on the Ser112 gatekeeper site. FEBS Lett 2004;571: 43-9.

29. Amaravadi R, Thompson CB. The survival kinases Akt and Pim as potential pharmacological targets. J Clin Invest 2005;115: 2618-24.

30. Zhang Y, Wang Z, Li X, Magnuson NS. Pim kinase-dependent inhibition of c-Myc degradation. Oncogene 2008;27: 4809-19.

31. Coller HA, Grandori C, Tamayo P, Colbert T, Lander ES, Eisenman RN*, et al.* Expression analysis with oligonucleotide microarrays reveals that MYC regulates genes involved in growth, cell cycle, signaling, and adhesion. Proc Natl Acad Sci U S A 2000;97: 3260-5.

32. Bouchard C, Thieke K, Maier A, Saffrich R, Hanley-Hyde J, Ansorge W*, et al.* Direct induction of cyclin D2 by Myc contributes to cell cycle progression and sequestration of p27. EMBO J 1999;18: 5321-33.

33. Perez-Roger I, Solomon DL, Sewing A, Land H. Myc activation of cyclin E/Cdk2 kinase involves induction of cyclin E gene transcription and inhibition of p27(Kip1) binding to newly formed complexes. Oncogene 1997;14: 2373-81.

34. van der Lugt NM, Domen J, Verhoeven E, Linders K, van der Gulden H, Allen J*, et al.* Proviral tagging in E mu-myc transgenic mice lacking the Pim-1

proto-oncogene leads to compensatory activation of Pim-2. EMBO J 1995;14: 2536-44.

35. Mikkers H, Allen J, Knipscheer P, Romeijn L, Hart A, Vink E*, et al.* High-throughput retroviral tagging to identify components of specific signaling pathways in cancer. Nat Genet 2002;32: 153-9.

36. Abe M. Targeting the interplay between myeloma cells and the bone marrow microenvironment in myeloma. Int J Hematol 2011;94: 334-43.

37. Chiles TC. Regulation and function of cyclin D2 in B lymphocyte subsets. J Immunol 2004;173: 2901-7.

38. Ohtsubo M, Theodoras AM, Schumacher J, Roberts JM, Pagano M. Human cyclin E, a nuclear protein essential for the G1-to-S phase transition. Mol Cell Biol 1995;15: 2612-24.

39. Baudino TA, Cleveland JL. The Max network gone mad. Mol Cell Biol 2001;21: 691-702.

40. Danial NN. BAD: undertaker by night, candyman by day. Oncogene 2008;27 Suppl 1: S53-70.

41. Chen LS, Redkar S, Bearss D, Wierda WG, Gandhi V. Pim kinase inhibitor, SGI-1776, induces apoptosis in chronic lymphocytic leukemia cells. Blood 2009;114: 4150-7.

42. Hay N, Sonenberg N. Upstream and downstream of mTOR. Genes Dev 2004;18: 1926-45.

43. Ma XM, Blenis J. Molecular mechanisms of mTOR-mediated translational control. Nat Rev Mol Cell Biol 2009;10: 307-18.

44. Chen LS, Redkar S, Taverna P, Cortes JE, Gandhi V. Mechanisms of cytotoxicity to Pim kinase inhibitor, SGI-1776, in acute myeloid leukemia. Blood 2011;118: 693-702.

45. Yaccoby S. Advances in the understanding of myeloma bone disease and tumour growth. Br J Haematol 2010;149: 311-21.

46. Sonmez M, Akagun T, Topbas M, Cobanoglu U, Sonmez B, Yilmaz M*, et al.* Effect of pathologic fractures on survival in multiple myeloma patients: a case control study. J Exp Clin Cancer Res 2008;27: 11.

## FIGURE LEGENDS

**Figure 1. MM cells express PIM kinases and are sensitive to the anti-proliferative effect of the pan-PIM kinase inhibitor, PIM447. (a)** Basal protein levels of PIM1, PIM2 and PIM3 were analyzed by Western blot in 10 MM cell lines. α-tubulin was used as a loading control. **(b)** Basal gene expression of PIM1, PIM2 and PIM3, assessed by the Human gene 1.0 ST array (Affymetrix) in CD138+ myeloma cells isolated from 41 patients with MM. Normalized expression intensity was calculated as described in the Material and Methods. An outlier at a distance of greater than 1.5x the interquartile range from the box is plotted individually as a dot. Global differences among groups were evaluated by the Kruskal–Wallis test; significant pair-wise differences were identified by the Mann-Whitney U test. All the p-values were adjusted for multiple comparisons using the False Discovery Rate (FDR) method (***$P$ <0.001). **(c)** The indicated MM cell lines were incubated with increasing concentrations of PIM447 for 24, 48 and 72 hours and cell viability was analyzed by MTT assay. The average absorbance values of control untreated samples were taken as

100%. Data are summarized as the mean ± SD (n=3) **(d)** $IC_{50}$ values for PIM447 at 48 hours were plotted against PIM1, PIM2 and PIM3 expression as measured by Western blot and normalized with α-tubulin using the image processing package Fiji. r=Pearson correlation coefficient; *p*=p-value.

**Figure 2. PIM447 induces apoptosis and cell cycle arrest in MM cells and overcomes the resistance conferred by MSCs and OCs**. **(a)** MM1S, NCI-H929, RPMI-8226, OPM-2 and RPMI-LR5 cells were treated with increasing doses (0.1-10 μM) of PIM447 for 24 and 48 hours, and the induction of apoptosis was analyzed by flow cytometry after annexin-V staining. Data represent the percentage of apoptotic cells for each condition after subtracting the basal percentage of apoptotic cells for each cell line **(b)** MM1S cells were treated with 10 μM PIM447 for the indicated times, and the induction of apoptosis was analyzed by flow cytometry. Data are summarized as the mean ± SEM (n=3). Statistically significant differences between control (0 h) and different time points are represented as ****P* <0.001, ***P* <0.01 and **P* <0.05 (Student's t-test) **(c)** MM1S cells were treated with 10 μM PIM447 for the indicated times, and the expression of caspase 8, caspase 9, caspase 3, caspase 7 and PARP was analyzed by Western blot using α-tubulin as loading control. **(d)** MM1S and OPM-2 cells were incubated with increasing concentrations of PIM447 for 48 hours, and the cell cycle profile was examined by flow cytometry, as shown by representative histograms. Tables refer to one experiment that was repeated twice with similar results in the two cell lines and indicate the percentage of cells in $subG_0$ (apoptotic cells) and the percentages in $G_0$-$G_1$, S and $G_2$-M from the non-$subG_0$ population. **(e)** Freshly isolated BM cells obtained from 10 patients with MM were treated *ex vivo* with increasing

concentrations of PIM447 for 48 hours. After the incubation period, cells were stained with the combination of annexin V-FITC and three monoclonal antibodies (CD56-PE, CD45-PerCP-Cy5.5 and CD38-APC) for the analysis of apoptosis in myeloma cells and lymphocytes. Outliers further than 1.5x or 3x the interquartile range from the box are plotted individually as dots and asterisks, respectively. **(f)** MM1S-luc cells were co-cultured with the hMSC-TERT cell line for 2 days or pre-OCs derived from healthy donors for 5 days with the indicated concentrations of PIM447 and under low-serum conditions. After the co-culture period, MM1S-luc growth was assessed by luciferase bioluminescence measurement. Graphs illustrate the mean ± SD (n=3).

**Figure 3. PIM447 synergizes with different anti-myeloma agents in the MM1S cell line.** MM1S cells were treated with the indicated double or triple combinations of PIM447, dexamethasone and either **(a)** bortezomib for 48 hours, **(b)** lenalidomide for 72 hours or **(c)** pomalidomide for 72 hours. Cell viability was analyzed by MTT assay as represented in the graphs.

**Figure 4. Effect of PIM447 on PIM kinase-related targets.** MM1S or OPM-2 cells were treated with 10 μM PIM447 for the indicated times and the expression of different proteins was analyzed by Western blot. Alpha-tubulin was used as a loading control. **(a)** Protein levels of phospho-Bad (Ser112), total Bad, Bcl-2, Bcl-xl and Mcl-1 in MM1S. **(b)** The levels of phospho-TSC2 in MM1S were analyzed by immunoprecipitation of TSC2 with an anti-TSC2 antibody and subsequent immunoblotting with a phospho-Akt substrate antibody. The expression of total TSC2, phospho PRAS40 (Thr246), total PRAS40, phospho 4EBP1 (Thr 37/46), total 4EBP1, phospho P70S6 (Thr 389), total P70S6, phospho S6RP (Ser 235/236) and total S6RP were analyzed by

Western blot. **(c)** Protein levels of total c-Myc, phospho-c-Myc (Ser 62), Mad-1, cyclin D2 and cyclin E1 in MM1S. **(d)** Protein levels of phospho-Bad (Ser112), total Bad, c-Myc and phospho-c-Myc (Ser 62) in OPM-2. **(e,f)** $IC_{50}$ values for PIM447 at 48 hours were plotted against Bad and phospho-Bad expression, respectively, as measured by Western blot and normalized with α-tubulin using the image processing package Fiji. r=Pearson correlation coefficient; *p*=p-value.

**Figure 5. PIM447 inhibits *in vitro* OC formation and resorption and increases OB differentiation and activity. (a)** PBMCs were differentiated in osteoclastogenic medium for the indicated times. PIM1, PIM2 and PIM3 expression was analyzed by Western blot. **(b)** OC formation was evaluated by the mean number of TRAP+ multinucleated cells (≥3 nuclei) per well after PIM447 treatment of osteoclastogenic cultures for 21 days. Half-maximal inhibitory concentration ($IC_{50}$) of PIM447 was calculated using SigmaPlot graphing software. Data are summarized as the mean ± SEM. Representative micrographs of TRAP+ OCs are shown. Bar=50 μm. **(c)** To test the effect of PIM447 on OC resorption, inhibition of matrix mineralization was assessed by PBMCs cultured on calcium-coated slices in the presence of osteoclastogenic medium and PIM447 treatment as indicated. After 17 days, OCs were removed and the area of resorbed lacunae analyzed. Data are summarized as the mean ± SEM. Representative micrographs of resorptive pits after PIM447 treatment are reported. Bar=50 μm. Statistically significant differences *versus* vehicle control in b and c were identified by the Mann–Whitney U test (* $P$ <0.05). **(d)** PBMCs were differentiated in osteoclastogenic medium and exposed to different concentrations of PIM447. The levels of PU.1, phospho Erk1/2 and NFATc1 at day 7 and Cathepsin K at day 14 were analyzed by Western blot,

using α-tubulin as a loading control. **(e)** Pre-OCs differentiated under PIM447 exposure for 14 days were stained with rhodamine-conjugated phalloidin and examined by fluorescence microscopy to visualize the F-actin ring. Representative micrographs are shown. Bar = 50 µm. **(f)** Normalized gene expression of several molecules implicated in OC resorption [*MMP9* (matrix metalloproteinase 9), *ATP6V1A* (vacuolar-$H^+$-ATPase catalytic subunit A1) and *CA2* (carbonic anhydrase II)] after osteoclastogenic differentiation of PBMCs for 21 days in the presence of PIM447 (2.5 µM), was assessed by real-time RT-PCR. Relative gene expression was calculated by the $2^{-\Delta Ct}$ method, where $\Delta Ct$ = Ct (gene) – Ct (GAPDH). Results are expressed as the mean ± SEM. Significant differences with respect to control were assessed with the Student's t-test (* $P$ <0.05). **(g)** Primary bone marrow MSCs from myeloma patients (n=5) were maintained in osteogenic medium in the presence of indicated PIM447 concentrations, and ALP activity (nM/min/µg protein) was measured at day 11. Results are expressed as mean ± SEM (** $P$ <0.01 *versus* control, calculated by the Mann-Whitney test) **(h)** Representative micrographs of matrix mineralization by Alizarin Red staining in OBs derived from MSCs from a MM patient (21 days of osteogenic differentiation in the presence of PIM447).

**Figure 6. Oral administration of PIM447 decreased tumor burden and prevented myeloma-associated bone loss in a mouse model of disseminated MM.** RPMI-8226-luc cells (8 x $10^6$) were intravenously injected into NSG mice. After 4 weeks, mice were randomized into two groups (receiving vehicle or PIM447; n=12/group), and treated with dosing and regimen schedules as specified. Orally delivered PIM447 effectively reduced tumor burden as measured by BLI **(a)** and serum levels of human Igλ secreted by

RPMI-8226-luc cells **(b)**. Data (a and b) are summarized as the mean ± SEM. In a, * (*P* <0.05) represents the first day in which differences with respect to vehicle were statistically significant. In b, ****P* <0.001 *versus* vehicle. **(c)** Representative microCT cross-sections at the metaphysis of distal femurs show loss of trabecular architecture in vehicle mice with MM, whereas PIM447-treated mice retain a trabecular microarchitecture similar to that of normal bone (mice not injected with myeloma cells; n=4). **(d)** PIM447 significantly increased bone parameters of bone volume density and trabecular number, whereas trabecular separation was decreased. Results are summarized as the mean ± SEM. Global differences among the three groups were evaluated with the Kruskal–Wallis test while pairwise comparisons were evaluated with the Mann-Whitney U test. All the p-values were adjusted for multiple comparisons using the False Discovery Rate (FDR) method: **P* <0.05, ***P* <0.01 and n.s.=not significant. **(e)** PIM447 significantly reduced serum levels of the bone resorption marker CTX. **P* <0.05 *versus* vehicle (Student's t-test). **(f)** PIM447 also augmented serum levels of the bone formation marker P1NP with respect to vehicle-treated mice, although this change was not found to be significant (*P* = 0.06, calculated with the Student´s t-test). Data are expressed as the mean ± SD (e and f).

Author Manuscript Published OnlineFirst on July 20, 2016; DOI: 10.1158/1078-0432.CCR-16-0230
Author manuscripts have been peer reviewed and accepted for publication but have not yet been edited.

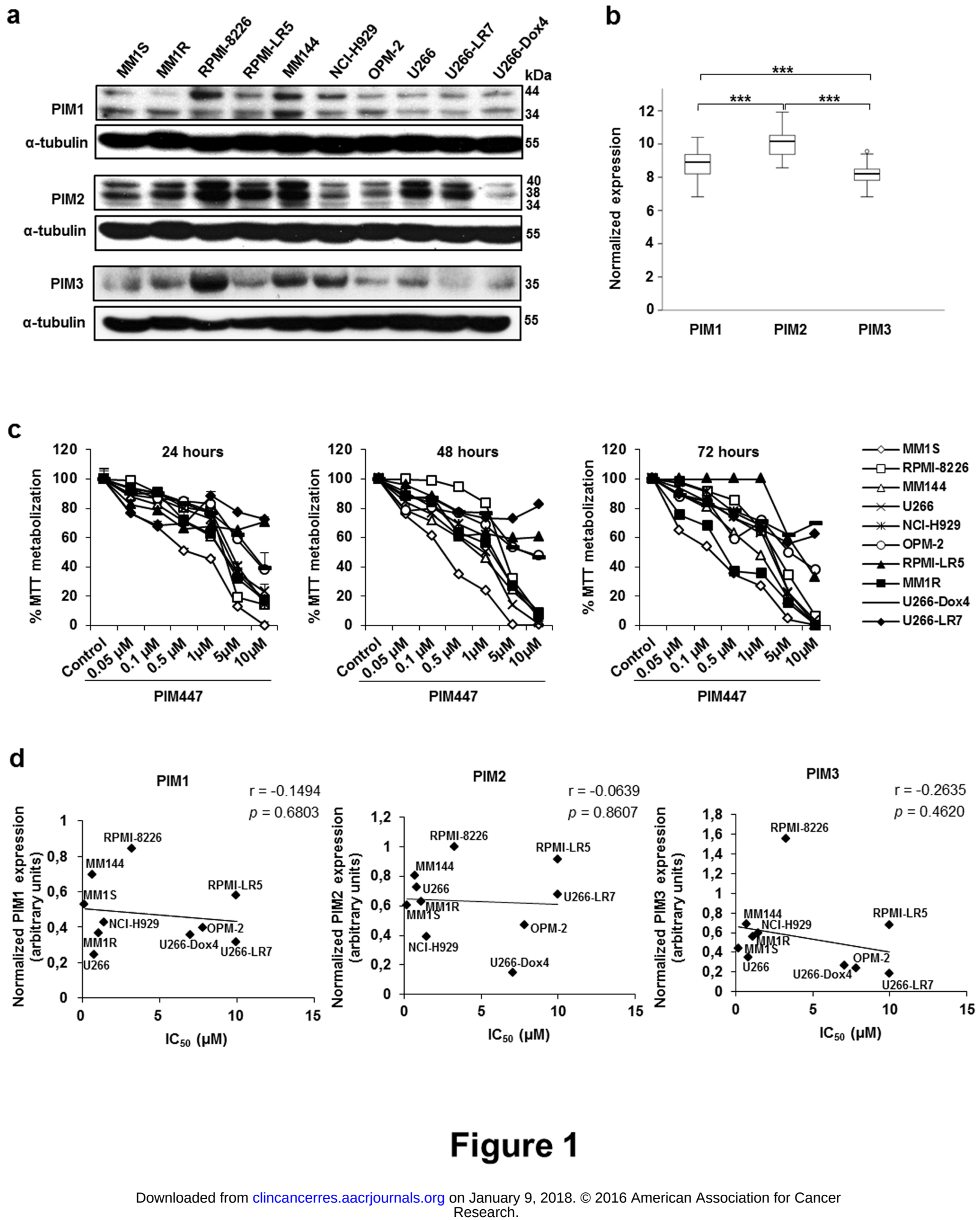


# Figure 1

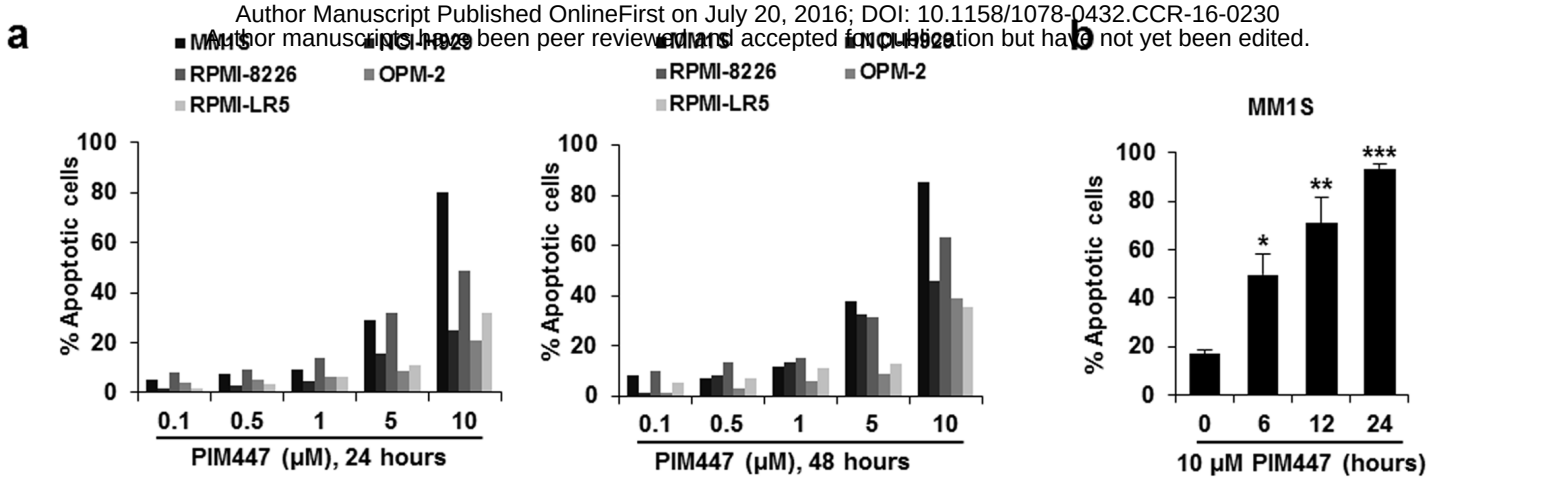


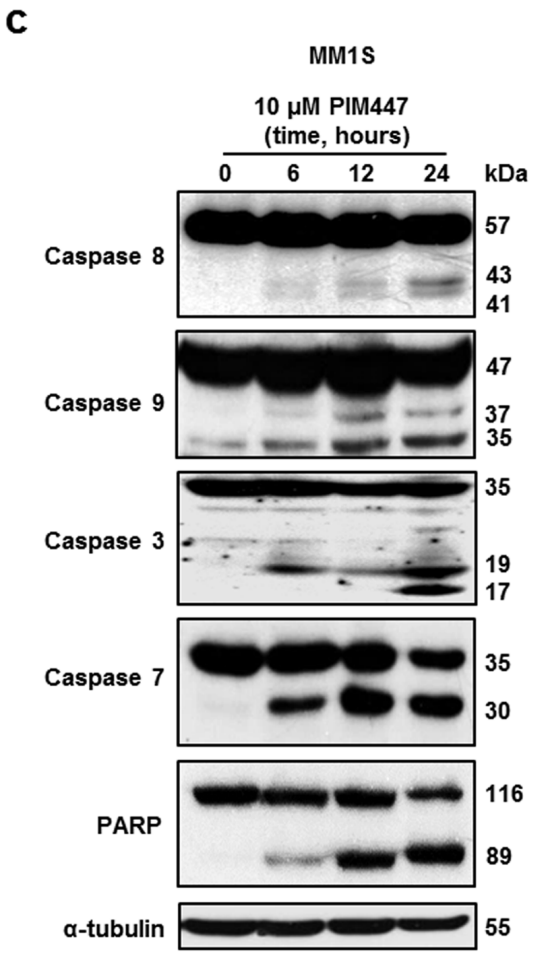


d

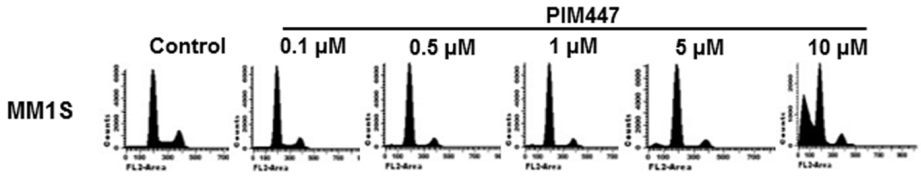


| | | | | | | |
|---|---|---|---|---|---|---|
| SubG$_0$ | 2 | 2,74 | 4,59 | 4,88 | 7,41 | 47,36 |
| G$_0$-G$_1$ | 66,59 | 76,79 | 83,25 | 85,77 | 86 | 79,99 |
| S | 15,27 | 9,67 | 5,61 | 3,5 | 3,22 | 4,95 |
| G$_2$-M | 18,14 | 13,54 | 11,14 | 10,73 | 10,78 | 15,06 |

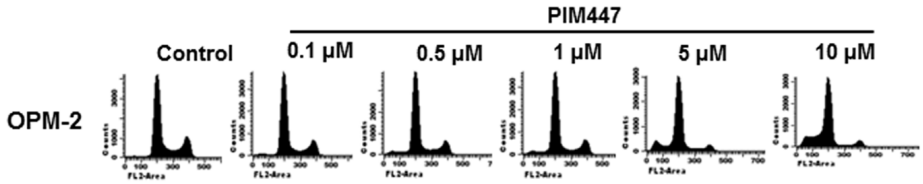


| | | | | | | |
|---|---|---|---|---|---|---|
| SubG$_0$ | 3,69 | 4,93 | 8,79 | 9,15 | 21,86 | 30,37 |
| G$_0$-G$_1$ | 56,49 | 63,03 | 67,58 | 66 | 75,29 | 80,23 |
| S | 24,33 | 22,33 | 18,4 | 18,74 | 15,31 | 10,88 |
| G$_2$-M | 19,19 | 14,64 | 14,01 | 15,26 | 9,4 | 8,9 |

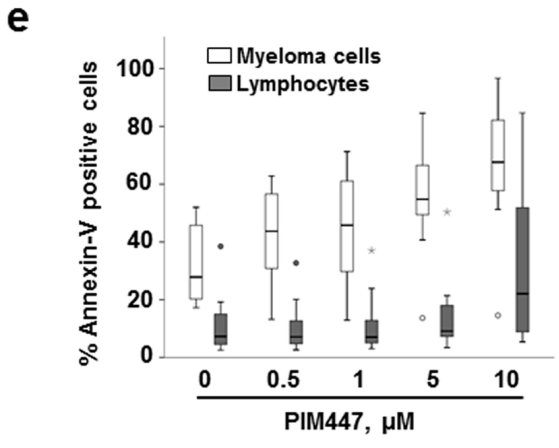


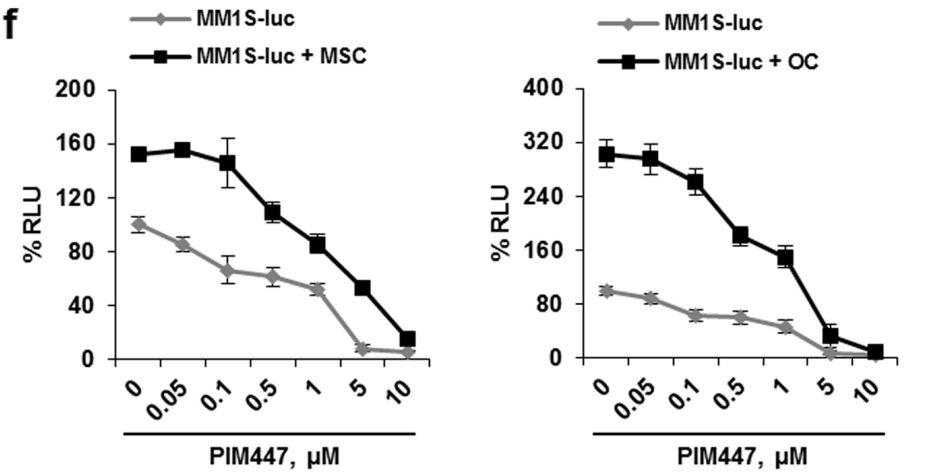


**Figure 2**

Author Manuscript Published OnlineFirst on July 20, 2016; DOI: 10.1158/1078-0432.CCR-16-0230
Author manuscripts have been peer reviewed and accepted for publication but have not yet been edited.

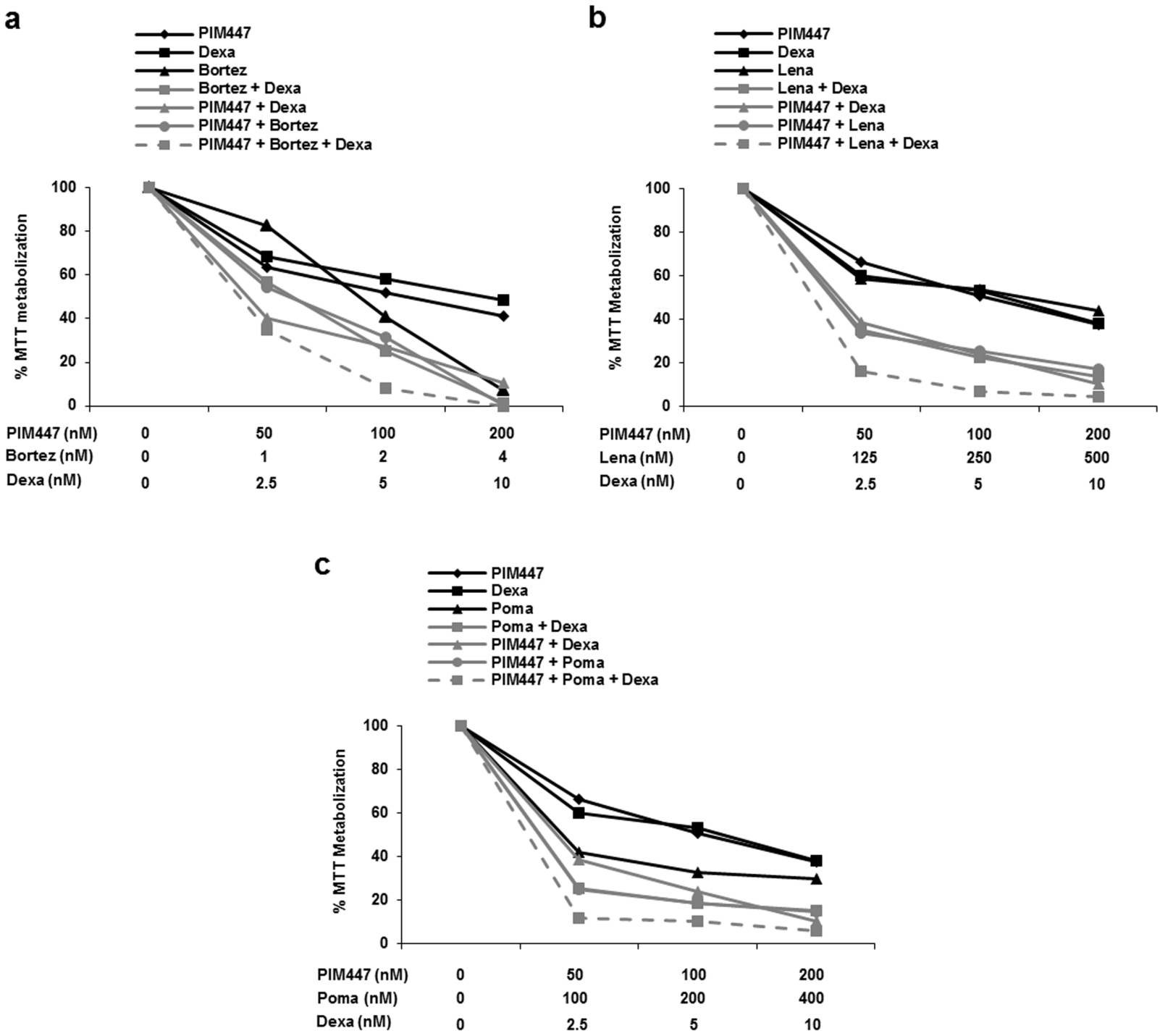


# Figure 3

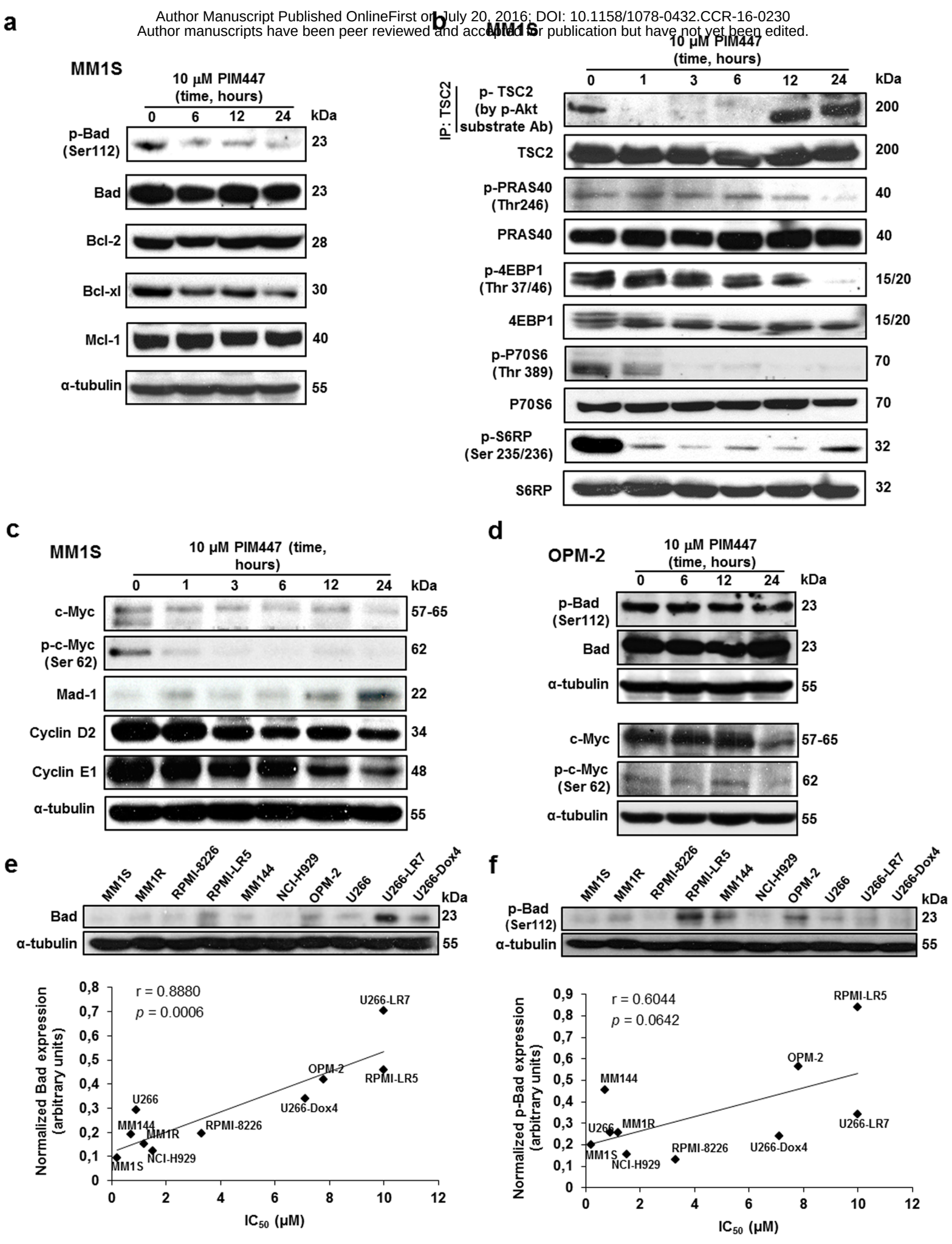


**Figure 4**

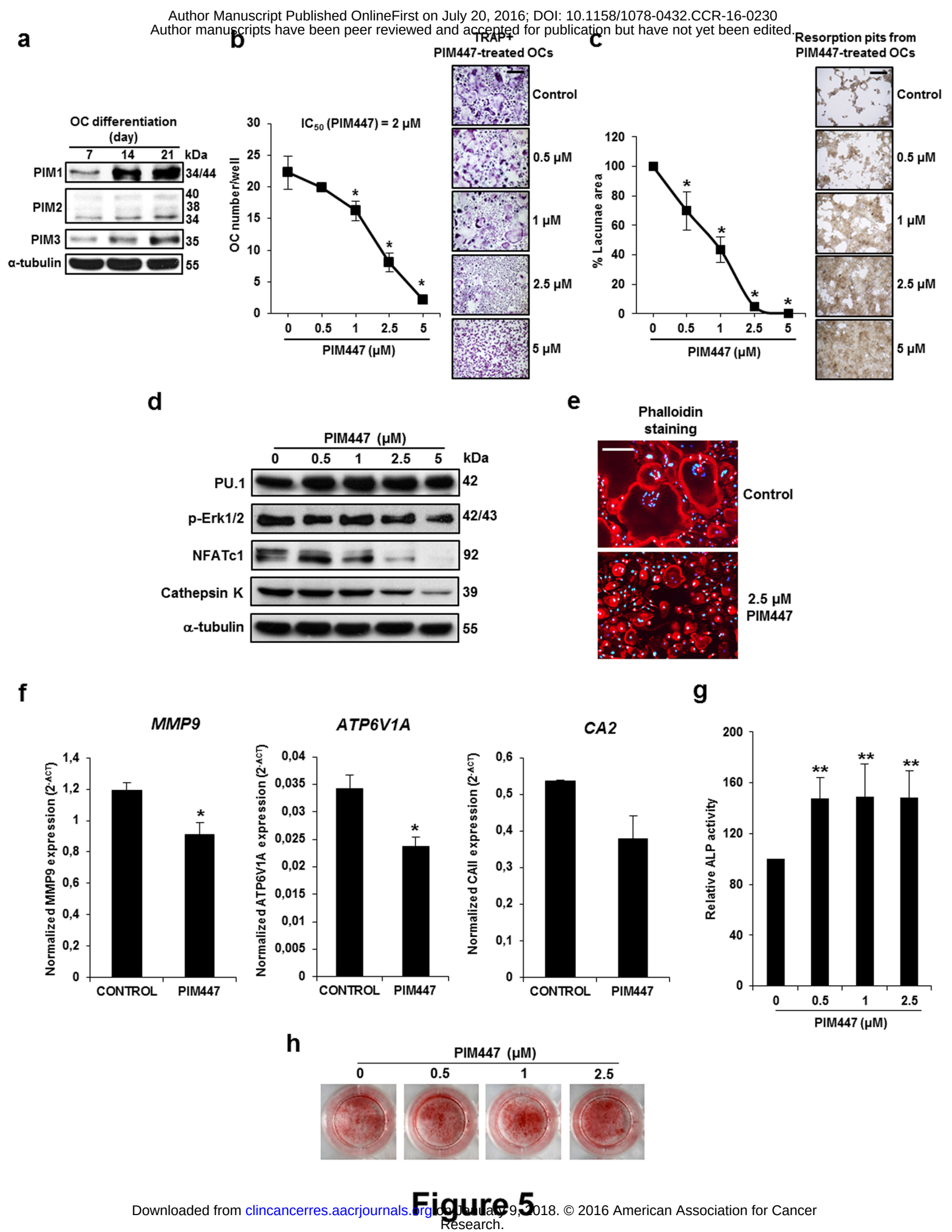


**Figure 5**

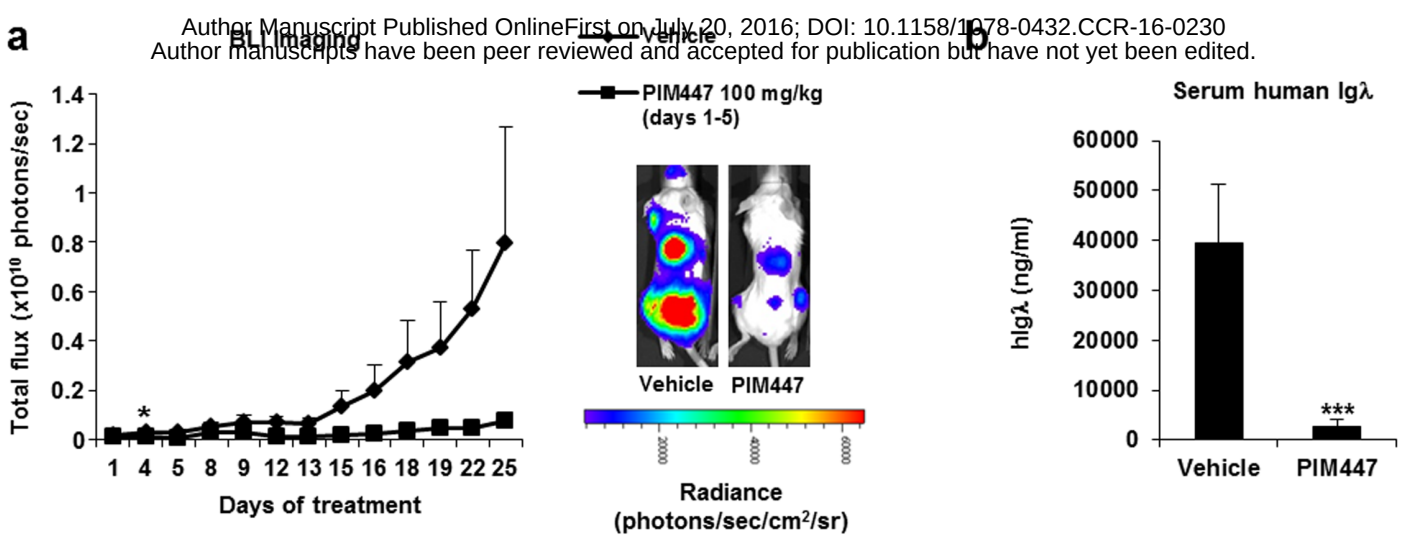


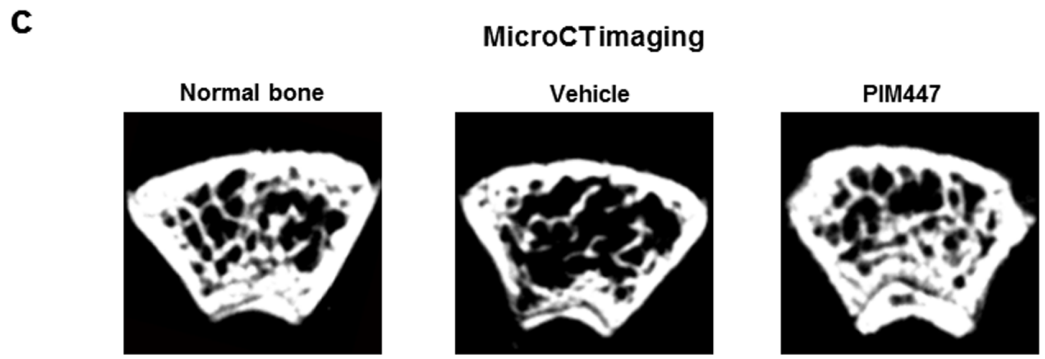


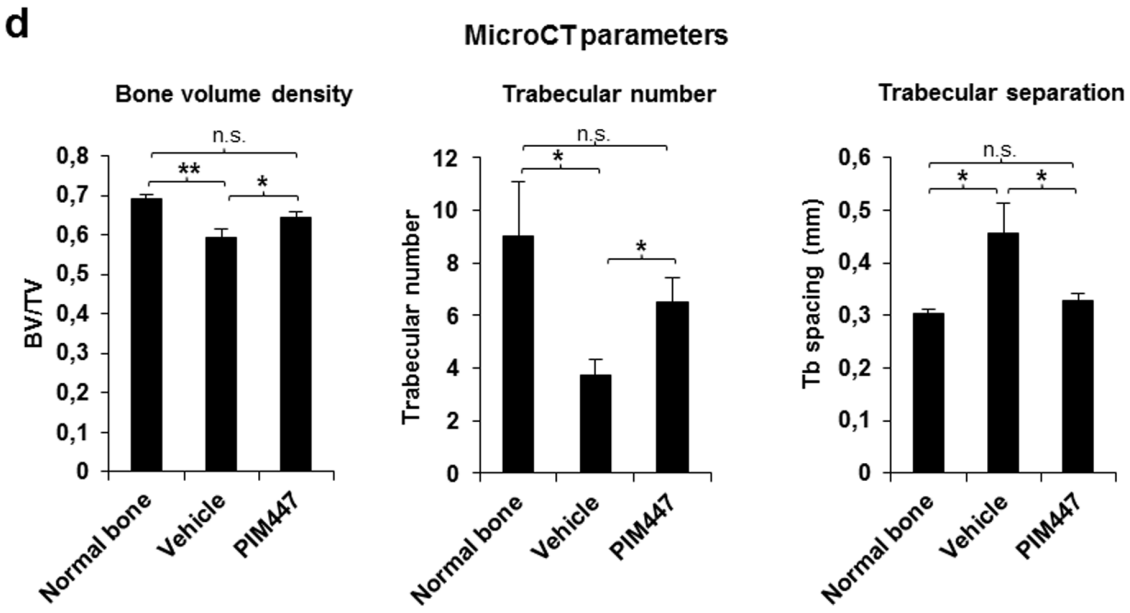


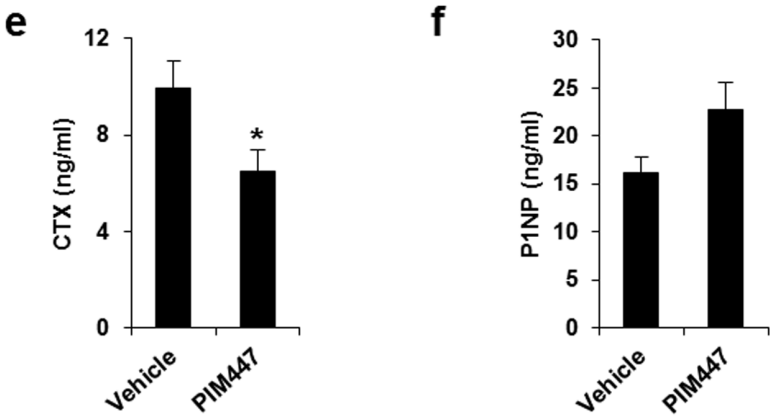


**Figure 6**

AACR American Association for Cancer Research

Clinical Cancer Research

# The novel pan-PIM kinase inhibitor, PIM447, displays dual anti-myeloma and bone protective effects, and potently synergizes with current standards of care

Teresa Paíno, Antonio García-Gómez, Lorena González-Méndez, et al.

*Clin Cancer Res* Published OnlineFirst July 20, 2016.